Atmos. Chem. Phys. Discuss., 9, 22581–22617, 2009
www.atmos-chem-phys-discuss.net/9/22581/2009/

Atmospheric
Chemistry
and Physics
Discussions

Peroxyacetic acid in urban and rural atmosphere: concentration, feedback on PAN$-$NO$_x$ cycle and implication on radical chemistry

X. Zhang, Z. M. Chen, S. Z. He, W. Hua, Y. Zhao, and J. L. Li

State Key Laboratory of Environmental Simulation and Pollution Control, College of Environmental Sciences and Engineering, Peking University, Beijing 100871, China

Received: 2 October 2009 – Accepted: 8 October 2009 – Published: 26 October 2009

Correspondence to: Z. M. Chen (zmchen@pku.edu.cn)

Published by Copernicus Publications on behalf of the European Geosciences Union.

Abstract

Peroxyacetic Acid (PAA) is one of important atmospheric organic peroxides, which have received increasing attention for their potential contribution to the oxidation capacity of the troposphere and the formation of secondary aerosols. We report here that, for the first time, a series of data for atmospheric PAA concentrations at urban and rural sites, from five field campaigns carried out in China in summer 2006, 2007 and 2008. For these five measurements, daytime mean PAA concentrations on sunlit days were 0.02–0.14 ppbv with a maximum level of ~1 ppbv. The various meteorological and chemical parameters influencing PAA concentrations were examined using the Principal Factor Analysis. This statistical analysis shows that the local photochemical production was the major source of PAA, and its concentration increased with increasing temperature, solar radiation and ozone but decreased with increasing NO_x (NO and NO_2), CO, SO_2, and relative humidity. Based on the dataset, several issues are highlighted in this study: (i) because PAA is a product from the photochemical oxidation of some specific volatile organic compounds (VOCs) that lead to acetyl peroxy radicals, the importance of various VOCs with respect to the PAA formation is therefore ranked using the incremental reactivity method. (ii) The contribution of PAN thermal degradation to PAA formation under conditions of different NO_x concentrations is estimated based on the chemical kinetics analysis. The result shows that PAN seems to play an important role in the formation of PAA when the NO/NO_2 concentration ratio was less than 0.2 and PAA would correspondingly have feedback on the PAN−NO_x cycle. (iii) PAA and other peroxides, such as methyl hydroperoxide (MHP) and H_2O_2, usually exhibited a similar asymmetric shape typically shifted to the afternoon. However, at a high SO_2 level, H_2O_2 showed a profile different from those of MHP and PAA. The combination of linear regression and chemical kinetics analysis reveals that a possible unknown pathway results in the significant removal of H_2O_2 and the extent of H_2O_2 undergoing this pathway needs a further study. (iv) Considering that PAA is the reservior of free radicals, its fate is expected to have an effect on the free radical budget in the atmosphere. A box model

based on the CBM-IV mechanism has been performed to access its influence on the radical budget. We suggest that the detailed information on PAA in the atmosphere is of importance to better understand the free radical chemistry.

1 Introduction

Peroxyacetic acid (PAA) plays a potentially important role in atmospheric processes. As an organic peroxide oxidant, PAA contributes to the oxidation capacity of the atmosphere (Barth et al., 2007; Acker et al., 2008) and the formation of secondary sulfate (Lind et al., 1987; Stockwell et al., 1994); as a reservoir of free radicals, PAA can reflect the free radical levels of the troposphere and indicate the extent of free radical chemistry involved at a particular location (Jackson and Hewitt, 1999; Lee et al., 2000). Furthermore, PAA is thought to have some toxic effects on ecosystem and human beings.

No significant direct emission of PAA from natural or anthropogenic sources has been found, and it is believed that the atmospheric PAA is mainly produced through the combination of peroxy radicals (Reactions R1, R2) (Lightfoot et al., 1992; Staffelbach et al., 1995). Besides, A small amount of PAA can be formed by the reaction of acetyl peroxy radical ($CH_3C(O)OO$) with high concentrations of “H-atom donors” commonly found in atmospheric aqueous phase, like formate, formaldehyde, glyoxal and phenolic compounds (Reaction R3) (Faust et al., 1997). The sink of PAA includes photolysis, reaction with the hydroxy radical (OH), and loss by physical deposition to the ground (Reactions R4, R5) (Jackson and Hewitt, 1999). The photolysis of PAA releases OH (Keller et al., 2008), and the reaction between PAA and OH regenerates $CH_3C(O)OO$ (Jenkin et al., 1997), so that PAA is involved in the radical balance as both a source and a sink.

$$CH_3C(O)OO^{\cdot} + HO_2^{\cdot} \rightarrow CH_3C(O)OOH + O_2 \tag{R1}$$

$$CH_3C(O)OO^{\cdot} + CH_3OO^{\cdot} \rightarrow CH_3C(O)OOH + HCHO + O_2 \tag{R2}$$

$$CH_3C(O)OO^{\cdot} + RH \rightarrow CH_3C(O)OOH + R^{\cdot} \qquad (R3)$$

$$CH_3C(O)OOH + \nu \rightarrow CH_3C(O)O^{\cdot} + {}^{\cdot}OH \qquad (R4)$$

$$CH_3C(O)OOH + {}^{\cdot}OH \rightarrow CH_3C(O)OO^{\cdot} + H_2O \qquad (R5)$$

In recent years, PAA has been widely used in industry for disinfection and bleaching purposes. In many industrial and medical applications, a release of PAA can not be fully avoided (Henneken et al., 2006). It has been found that high exposure and eye contact will cause severe health problems. For the above reasons, many studies were focusing on developing reliable and commercial methods to detect its aqueous concentration (Davies and Deary, 1988; Pinkernell et al., 1996; Ruttinger and Radschuweit, 2000; Awad et al., 2003), and to monitor its airborne concentration on a regular basis in workplace environments (Effkemann et al., 1999; Hecht et al., 2004; Henneken et al., 2006). However, there has been comparatively few reported field observations of PAA (Fels and Junkermann, 1993; Walker et al., 2006), and the measurement database for its concentration in the atmosphere is incomplete.

In this paper, we focus on the less studied organic peroxide, PAA, by reporting its levels during five field campaigns carried out in urban and rural sites of China, namely, Beijing-2006, Beijing-2007, Beijing-2008, Backgarden-2006, and Mazhuang-2007. The primary aim of our study is fourfold: (i) to investigate the impact of meteorological and chemical factors on the concentrations and variations of PAA in the atmosphere; (ii) to examine the relationship between PAA and PAN using chemical kinetic analysis to elucidate the feedback of PAA on PAN–NO_x cycle; (iii) to provide new field evidence for potentially different sinks of three peroxides, namely, hydroperoxide, methyl hydroperoxide (MHP), and PAA, under the conditions of high SO_2 and relative humidity levels; and (iv) to evaluate the influence of PAA on free radicals budget using a box model based on the CBM-IV mechanism for better understanding the free radical chemistry.

2 Experimental

2.1 Measurement sites

Atmospheric PAA concentrations were investigated at three sites in China, namely, Peking University (PKU) campus in Beijing city (39.991° N 116.304°E), Mazhuang in Taian city, Shandong Province (36.150° N 116.133°E), and Backgarden in Guangzhou city, Guangdong Province (23.548° N 113.066°E), on the base of several regional integrated field campaigns, as shown in Fig. 1.

Beijing, the capital city of the country, is located in the north China. The PKU campus is in the northern downtown, which is the Silicon Valley of Beijing. The surroundings of campus are several electronic supermarkets, institutes, campuses, residential apartments and two major streets at its east and south which are often congested. The No. 4 subway line is under built at the east of the campus from 2006 to 2009. The sampling inlet was mounted on the roof of a six-story building (~26 m above ground). The PAA measurement was a part of air quality research campaign in Beijing (Beijing-2006, 2007, 2008) during 11 August–9 September 2006, 3–31 August 2007, and 11 July–31 August 2008. Beijing is located in temperate zone with half-moist continent monsoon climate and four distinct seasons. During the 2006 campaign, the average meteorological values (arithmetic mean±standard deviation) were: 26.1±4.6°C ambient temperature, 65.1±20.1% ambient relative humidity, 1002±5 hPa ambient pressure, 1.6±1.4 m/s local wind speed, and the dominant wind direction was southerly/westerly. During the 2007 campaign, the average meteorological values (arithmetic mean±standard deviation) were: 29.3±4.3°C ambient temperature, 54.0±15.3% ambient relative humidity, 1001±6 hPa ambient pressure, 1.5±0.8 m/s local wind speed, and the dominant wind direction was southerly/westerly. During the 2008 campaign, the average meteorological values (arithmetic mean±standard deviation) were: 28.1±5.6°C ambient temperature, 67.0±18.5% ambient relative humidity, 998±4 hPa ambient pressure, 1.0±0.9 m/s local wind speed, and the dominant wind direction was southerly.

Guangzhou, the capital city of Guangdong Province, is located in south China. As a megacity, the increase in industry and population impacts the air quality of Guangzhou and this city is undergoing the complex air pollution due to the mixture of coal burning and vehicle emissions. Backgarden is a rural site, surrounded by 20 km^2 of forest and 2.7 km^2 of lake, located in the north of the central Pearl River Delta Region (PRD) and about 60 km northwest of Guangzhou. Backgarden is a much less populated area at the outskirts of the densely populated center of the PRD and can be treated as a regional background site. Backgarden does not have significant local vehicle emission, while the biomass burning in the afternoon and cable burning in the evening might be a source of locale mission. The sampling inlet was mounted on the roof of a three-story hotel building (~14 m above ground), which is located next to a 2.7 km^2 reservoir in a rural resort surrounded by a large area of farmland and forest. The PAA measurement was a part of Program of Regional Integrated Experiments of Pearl River Delta Region (PRIDE-PRD) during 3–30 July 2006. The Backgarden site experiences a typical sub-tropical climate and is usually influenced by the monsoon circulation in July. During the period of PAA measurement, the observation site was mainly influenced by the western pacific subtropical high pressure and typhoon. When controlled by the western pacific subtropical high pressure from 19 to 23 July, the days were sunny, and the dominant wind direction at Backgarden was southerly. When influenced by typhoon from 24 to 25 July, northerly winds prevailed at the observation site. During the last days of campaign from 26 to 30 July, the local weather conditions were cloudy and rainy and the sampled air masses came mainly from the south/southeast. The average meteorological values (arithmetic mean±standard deviation) for the campaign were: 29.5±3.4°C ambient temperature, 76.2±14.4% ambient relative humidity, 1001±4 hPa ambient pressure, and 1.9±1.2 m/s local wind speed.

Mazhuang is a rural site located 40 km southwest of Taian, a middle city in Shandong province, northeast of China. Taian city, the location of Mount Tai, is suffering from the acid rain pollution in recent years and the amount of rain of pH≤4.5 accounted for nearly 16% of total precipitation every year. The sampling inlet was mounted on the roof of a container (~5 m above the ground) on the playground of a primary school. It was surrounded by farmland and a national highway passed by there 1 km north. The PAA measurement was a part of China atmospheric acidifying mechanism research campaign carried out during 29 June–31 July 2007. Mazhuang experiences half-moist continent monsoon climate. During the observation period, the average meteorological values (arithmetic mean ± standard deviation) were: 28.7±5.8°C ambient temperature, 70.4±19.6% ambient relative humidity, 1001±5 hPa ambient pressure, 1.2±1.3 m/s local wind speed, and the dominant wind direction was southerly/southeasterly.

2.2 Measurement method for PAA

2.2.1 Instrument

For the five measurements, an automatically gound-based apparatus for hydrogen peroxide and organic peroxides measurement was set up by using a scrubbing coil collector to sample ambient air. High performance liquid chromatography (HPLC) post-column derivatization equipped with fluorescence detection was used for the analysis of PAA and other peroxides, The details about this instrument can be found in our previous work (Xu and Chen, 2005; Hua et al., 2008). The instrument was located in an air conditioned room or container and the sampling inlet was mounted on the rooftop of the building or container. The detection limits for atmospheric H_2O_2 and organic peroxides were usually in the range of 10–30 pptv.

2.2.2 Chemicals

H_2O_2 was purchased from Sigma-Aldrich (35% solution). PAA was synthesized from H_2O_2 and acetic acid (>99.5%, Damao), and methyl hydroperoxide was synthesized from H_2O_2 and dimethyl sufate as described in Hua et al. (2008). The concentrations of stock solutions and standard solutions were determined using $KMnO_4$ and $KI/Na_2S_2O_3$/starch every two weeks. All reagents and standard solutions were prepared with 18 MΩ Milli-Q water (Millipore), and were stored at 4°C in a refrigerator.

2.3 Modeling methodology

A box model was performed based on the Carbon Bond Mechanism-Version IV (CBM-IV), developed by M. W. Gery (1989) and updated recently. The CBM-IV mechanism includes the degradation kinetics and oxidation schemes of 43 species. In this study, we add the PAA scheme into this mechanism based on parameters evaluated by Jenkin et al. (1997) and Atkinson et al. (1999). Typical model inputs include NO_x, SO_2, CO, VOCs, water vapor, and temperature. The box model calculations were carried out using initial VOCs and NO_x concentrations, with additional VOCs and NO_x emissions every 1-h during the 72-h simulations.

3 Results and discussion

3.1 General observations

Air samples for Beijing-2006, Beijing-2007, Beijing-2008, Backgarden-2006, and Mazhuang-2007 amounted to 862, 867, 2614, 354, and 1663, respectively. PAA was often present at several-decade pptv level, with a maximum value of ∼1 ppbv at Mazhang, 2007. In order to calculate the mean of the observed concentrations, any value below the detection limit was treated as zero. With regard to all samples, the mean (and standard deviation) concentrations during daytime (08:00–20:00 LT) were 0.03±0.04 ppbv for Beijing-2006, 0.11±0.13 ppbv for Beijing-2007, 0.03±0.05 ppbv for Beijing-2008, 0.02±0.05 ppbv for Backgarden-2006 and 0.14±0.20 ppbv for Mazhuang-2007. The mean values at night (20:00–08:00 LT) were 0.02±0.04 ppbv for Beijing-2006, 0.10±0.13 ppbv for Beijing-2007, 0.03±0.05 ppbv for Beijing-2008, 0.01±0.04 ppbv for Backgarden-2006 and 0.08±0.10 ppbv for Mazhuang-2007. These values are comparable with or exceeding those in previous measurements that PAA was occasionally detected with a concentration level of 0.1–0.3 ppbv (Walker et al., 2006) and accounted for less than 10% of total measured peroxides (Fels and Jundermann, 1993). Temporal profiles of PAA concentrations for the five campaigns are shown in Fig. 2. It is worth noting that (i) PAA levels in Mazhuang were much higher than those in Beijing and Backgarden; and (ii) for Beijing, PAA levels in 2007 were ~3 times on average higher than those in 2006 and 2008. For Mazhuang in 2007, the daytime NO concentration was very low, often less than 100 pptv, so that the scavenging amount of radicals by NO became less, leading to an accumulation of radicals and thus a high level of PAA. By comparing the meteorological data of the three measurements carried out in Beijing, we found that UV-B radiation in 2007 (the daily average values: 0.24–0.34 $\mathrm{W\,m^{-2}}$) was much higher than those in 2006 (the daily average values: 0.11–0.14 $\mathrm{W\,m^{-2}}$) and 2008 (the daily average values: 0.12–0.24 $\mathrm{W\,m^{-2}}$). Obviously, the elevated PAA level in 2007 can be attributed to the stronger solar radiation, which leads to a high radical yield.

The time series of PAA, H_2O_2 and MHP on 2 August 2008, a sunny day in Beijing, were shown in Fig. 3. The diurnal profile of PAA, which was similar to those of H_2O_2 and MHP, was consistent with the local photochemical production in a sunlit day. Throughout the night, there seemed to be no transportation from the residual layer and PAA was depleted even to under the detection limit at 04:00 LT. After sunrise, the photochemical production began and consequently, PAA concentration started to rise, reaching a maximum level at 17:00 LT. Its level remained relatively high in the afternoon and decayed slowly from the sunset to 24:00 LT.

3.2 Meteorological and chemical factors related to the ambient PAA level

A statistical method, Principal Factor Analysis (PFA) is employed in order to understand the influence of chemical and meteorological parameters on the PAA concentrations. The advantage of PFA is to provide the decomposition into modes of variation that can be more easily interpretable by performing dimensionality reduction (Jolliffe et al., 2002; Ren et al., 2009). A matrix with 12 variables, including PAA, SO_2, NO, NO_2, CO,

O_3, wind direction (WD), wind speed (WS), temperature (T), relative humidity (RH), total radiation (TI), and pressure (P), from 317 samples of Backgarden-2006 was analyzed. The varimax rotated factor pattern for the data set with 4 factors was arranged in descending order of variances explained, as shown in Table 1. Factor 1 was associated with the photochemical aged air-masses. As shown in Fig. 4, during 19–21 July, days were sunny with slight southern breeze, intense solar radiation, high temperature and low RH at noon. PAA exhibited a high concentration due to the continuous production of free radicals in the daytime. A delay between the maximum of solar radiation and PAA concentration was observed, for the reason that the production of peroxy radicals (HO_2) and $CH_3C(O)OO$ is the subsequent step following OH formation (Gnauk et al., 1997). It is not surprising for the positive correlation between temperature and PAA because temperature affects the reaction rate and the production of radicals in the atmosphere (Jackson and Hewitt, 1999; Reeves and Penkett, 2003). Factor 2 has a strong positive loading from SO_2 and NO_2, while a negative loading from PAA. The anti-correlation between PAA and these two primary pollutants can be derived from Fig. 5. PAA was present with high concentrations from midday to the late afternoon, while SO_2 and NO_2 remained relatively low levels. PAA had the ability to oxidize SO_2 in the aqueous phase (Lind et al., 1987), so it is possible that its reaction with SO_2 could contribute to the loss of PAA under the humid condition. The low NO_2 level condition is favorable for PAA production for the following two reasons: first, NO_2 provides a sink of OH; and second, NO_2 will compete for $CH_3C(O)OO$ with HO_2 in the atmosphere, producing peroxylacetyl nitrate (PAN). Therefore, PAA is inclined to accumulate to a high concentration when the ambient concentrations of SO_2 and NO_2 are low. Factor 3, which had a loading from PAA, wind speed, total radiation and pressure, indicates two possible sinks of PAA, namely, photolysis under an intense radiation and dry deposition under a shallow inversion and at a low wind speed. Previous studies have reported that the deposition rate of peroxide over trees is much higher than in the free troposphere (Walcek et al., 1987; Wesley et al., 1989). It is possible that dry deposition on the surface might act as an important sink for the loss of PAA in Backgarden, where natural

Title Page
Abstract Introduction
Conclusions References
Tables Figures
◂◂ ▸▸
◂ ▸
Back Close
Full Screen / Esc
Printer-friendly Version
Interactive Discussion

plants are luxuriant. Factor 4 has a strong loading from NO, suggesting that PAA levels are sensitive to the NO background. NO will compete directly with PAA production via the cross combination of RO_2 radicals if sufficient NO is present (Reactions R6, R7) (Frey et al., 2005). The NO suppression of radicals could be observed in the early morning of 24 July, when a spike in NO of over 20 ppbv possibly caused a reduction of PAA.

$$NO + HO_2^{\cdot} \rightarrow NO_2 + {}^{\cdot}OH \tag{R6}$$

$$CH_3C(O)OO^{\cdot} + CH_3OO^{\cdot} \rightarrow CH_3C(O)OOH + HCHO \tag{R7}$$

3.3 Correlations with other species

3.3.1 PAA and VOCs

PAA is produced from the photochemical oxidation of some volatile organic compounds (VOCs) which lead to $CH_3C(O)OO$. Here we refer to the maximum incremental reactivity (MIR) method (Carter and Atkinson, 1989; Grosjean et al., 2002) to evaluate the PAA formation potential (PFP).

$$PFP = \lim_{\Delta VOC_i \to 0} \left\{ \frac{PAA(VOC_i + \Delta VOC_i) - PAA(VOC_i)}{\Delta VOC_i} \right\},$$

where $PAA_{(VOC_i)}$ is the maximum of PAA calculated in the "base case" simulation, $PAA_{(VOC_i+\Delta VOC_i)}$ is the maximum of PAA calculated with the test VOC_i added in the "base case" simulation, and ΔVOC_i is the incremental change in the concentration of test VOC_i. The "base case" was the idealized simulation for urban atmosphere at $VOCs/NO_x$ ratio approaching 8:1. The initial concentrations of VOCs and NO_x represented their average values for Beijing-2006 (Xie et al., 2008). The chemical mechanism used to calculate PFP is CBM-IV. It is a lumped structure mechanism where organics are represented using 12 species (Dodge, 2000). PAR represents alkanes and most single-bonded carbon atoms found in other organics. Ethene is treated explicitly (as ETH); the C=C double bond in other 1-alkenes is represented using the OLE surrogate. Toluene is represented explicitly (as TOL) and the surrogate XYL is used to represent the dialkylbenzenes; the trialkylbenzenes are presented as 1 XYL+1 PAR. Formaldehyde is treated explicitly (as FORM); the carbonyl component of other aldehydes is represented using the surrogate ALD2 whose chemistry is similar to acetaldehyde. Isoprene is treated explicitly (as ISOP).

Figure 6 lists the percent contribution of each surrogate species to the total PFPs calculated by the MIR method. XYL was the most important species in terms of PAA formation, accounting for ~33% of the total PFPs. The VOCs represented by XYL surrogate mainly include dialkylbenzenes and trialkylbenzenes, whose oxidation in the atmosphere produces methylglyoxal and biacetyl that contain acetyl group (Obermeyer et al., 2009), therefore leading to PAA formation. Also important as precursor of PAA was the surrogate ISOP, accounting for ~18% of the total PFPs. Key products of isoprene, including methylglyoxal and pyruvic acid, undergoing further photochemical reactions in the atmosphere lead to $CH_3C(O)OO$. The surrogate OLE, representing alkenes, accounted for ~13% of the total PFPs. The oxidation of some alkenes, including propene, 2-butene and 2-pentene, produces acetaldehyde, as discussed below. FORM accounted for ~12% of the total PFPs, for the reason that the oxidation of formaldehyde gives HO_2. TOL accounted for ~9% of the total PFPs. Products of toluene oxidized by OH include methylglyoxal and HO_2. The PFP for ALD2 accounted for ~8% of the total PFPs, because the oxidation of acetaldehyde initiated by OH leads to CH_3CO and subsequently to $CH_3C(O)OO$. Other species, such as ETH and PAR (~6% and 3%, respectively, of the total PFPs), were less significant than other VOCs as precursors to PAA. The above analysis evaluates the photochemical reactivity of VOCs in terms of PAA formation. However, the observed PAA level in the atmosphere is not only dependent on the photochemical reactivity, but also the ambient concentration of each VOC. Taking Beijing-2006 field campaign as an example, the measurement results showed top 10 VOCs with relatively high concentrations were formaldehyde, acetaldehyde, toluene, benzene, isopentane, butane, dialkyl-benzenes, pentane, propane, and isoprene (Xie et al., 2008). Taking into account the photochemical reactivity of each VOC, we suggest that dialkylbenzenes, acetaldehyde, formaldehyde, and toluene were the key compounds in total VOCs contributing to the PAA formation in Beijing 2006.

3.3.2 PAA and PAN

As mentioned above, any reaction leading to CH_3CO or $CH_3C(O)OO$ will contribute to the PAA formation. It is well known that PAN is thermally unstable, decomposing to produce the acetyl peroxy radical and nitrogen dioxide (Orlando et al., 1992). Therefore, PAN, which has received attention as precursors to photochemically reactive species, including free radicals (Grosjean et al., 2002, 2003), should be an important precursor of PAA. In the absence of NO, we expect the concentration of PAA is associated with the extent of thermal degradation of PAN (Reactions R8, R9, R11), while under prevailing high NO conditions, PAA formation will be suppressed because $CH_3C(O)OO$ can be rapidly removed by NO (Reaction R10).

$$CH_3C(O)OO^{\cdot} + HO_2^{\cdot} \xrightarrow{k_8} CH_3C(O)OOH + O_2 \tag{R8}$$

$$CH_3C(O)OO^{\cdot} + NO_2 \xrightarrow{k_9} CH_3C(O)OONO_2 \tag{R9}$$

$$CH_3C(O)OO^{\cdot} + NO \xrightarrow{k_{10}} NO_2 + CO_2 + {}^{\cdot}CH_3 \tag{R10}$$

$$CH_3C(O)OONO_2 \xrightarrow{k_{11}} CH_3C(O)OO^{\cdot} + NO_2 \tag{R11}$$

Figure 7 presents the diurnal profiles of PAA and PAN at Backgarden on 24 July 2006. During that sunny day, the wind direction was northerly and veered to northwesterly in the afternoon, consistent with that of back trajectories obtained from NOAA (www. arl. noaa. gov), and the wind speed measured during daytime was ~2 m/s, ensuring that the transport distance of air mass was less than ∼30 km from sunrise to the afternoon. So we suggest that the variation of PAA and PAN concentrations can be attributed, to a large extent, to the local photochemical drive. It can be seen that the daytime level of PAA is one order of magnitude on average lower than that of PAN, suggesting that R9, which is highly dependent on the NO_2 concentration, is much more competitive than R8 in the atmosphere. The peak time of PAA is several hours later than that of PAN, for the reason that the thermal degradation of PAN produces $CH_3C(O)OO$, which will subsequently react with HO_2 to form PAA. To better understand the correlation between PAN and PAA, the loss rate of PAN and formation rate of PAA were examined, using the same data on 24 July as an example. From Reactions (R8–R11), rate laws for the destruction of PAN and the formation of PAA are given by:

$$-\frac{d[\mathrm{PAN}]}{d[t]} = k_9[\mathrm{CH_3C(O)OO\cdot}][\mathrm{NO_2}] - k_{11}[\mathrm{PAN}],$$

$$\frac{d[\mathrm{PAA}]}{d[t]} = k_8[\mathrm{CH_3C(O)OO\cdot}][\mathrm{HO_2\cdot}]$$

The steady-state equation for acetyl peroxy radical is

$$-\frac{d[\mathrm{CH_3C(O)OO\cdot}]}{d[t]} = -k_8[\mathrm{CH_3C(O)OO\cdot}][\mathrm{HO_2\cdot}] - k_9[\mathrm{CH_3C(O)OO\cdot}][\mathrm{NO_2}] \\ -k_{10}[\mathrm{CH_3C(O)OO\cdot}][\mathrm{NO}] + k_{11}[\mathrm{PAN}]=0$$

Substitution of this equation into PAN destruction and PAA formation equations gives the final answer:

$$-\frac{d\ln[\mathrm{PAN}]}{d[t]} = \frac{k_{10}k_{11}[\mathrm{NO}] + k_8k_{11}[\mathrm{HO_2\cdot}]}{k_8[\mathrm{HO_2\cdot}] + k_9[\mathrm{NO_2}] + k_{10}[\mathrm{NO}]};$$

$$\frac{d[\mathrm{PAA}]}{d[t]} = \frac{k_8k_{11}[\mathrm{HO_2\cdot}][\mathrm{PAN}]}{k_8[\mathrm{HO_2\cdot}] + k_9[\mathrm{NO_2}] + k_{10}[\mathrm{NO}]},$$

where [$HO_2\cdot$], [NO], [NO_2], and [PAN] are ambient concentrations measured, $k_8=4.3\times10^{-13}\exp(1040/T)$ cm^3 molecule^{-1} s^{-1}, $k_9=1.2\times10^{-11}\times(T/300)^{-0.9}$ cm^3 molecule^{-1} s^{-1}, $k_{10}=7.8\times10^{-12}\exp(300/T)$ cm^3 molecule^{-1} s^{-1}, and $k_{11}=5.4\times10^{16}\exp(-13\,830/T)$ s^{-1} (Atkinson et al., 1999). The results of the calculations are shown in Fig. 7. The PAN loss rate is not only dependent on temperature, but also on the NO/NO_2 concentration ratio because high NO concentrations enhance indirectly the thermal degradation of PAN (see Reactions R10 and R11), thereby preventing its recombination with NO_2 to form PAN (McFadyen and Cape, 2005). The PAA formation rate is a function of both HO_2 concentration and NO/NO_2 concentration ratio because although the thermal degradation of PAN increases with increasing NO/NO_2 concentration ratio at a given temperature, a high level of NO will compete with HO_2 for $CH_3C(O)OO$ produced by the thermal degradation of PAN. When the NO/NO_2 concentration ratio was approaching zero (09:50–10:30 LT), the loss rate of PAN and the formation rate of PAA were comparable. When NO/$NO_2\leq0.05$ and [HO_2]>20 pptv (10:30–11:00 LT), the loss rate of PAN was nearly ten times higher than the formation rate of PAA, suggesting that under low NO/NO_2 concentration ratio, the PAA formation is an important pathway to remove $CH_3C(O)OO$, thus accelerate the thermal degradation rate of PAN. When $0.05<$NO/$NO_2\leq0.2$ and [HO_2]>90 pptv (11:00–12:00 LT), the formation rate of PAA was ten times lower than the loss rate of PAN. It indicates that a certain amount of HO_2 will compete for $CH_3C(O)OO$ with NO_x, suppressing the reproduction of PAN and leading to an enhanced PAA level. When NO/$NO_2>0.2$, the loss rate of PAN was several orders of magnitude higher than the formation rate of PAA, even though the HO_2 concentration remained a high level and accordingly, the contribution of PAN thermal degradation to the PAA formation was considered to be minor. In conclusion, we suggest that under low NO/NO_2 concentration ratio conditions, the reaction between HO_2 and $CH_3C(O)OO$ will be significant, producing an enhanced level of PAA, which will correspondingly have feedback on the thermal decomposition of PAN.

Title Page
Abstract | Introduction
Conclusions | References
Tables | Figures
◀| |▶
◀ ▶
Back | Close
Full Screen / Esc
Printer-friendly Version
Interactive Discussion

3.3.3 PAA–H_2O_2–MHP relationship

As shown in Fig. 3, PAA generally presented the same diurnal profile as both H_2O_2 and MHP in a sunlit day, indicative of a similar photochemical formation mechanism of these three peroxides. However, the linear regression for data in July 2007 at Mazhuang, see Fig. 8, shows a weak positive correlation between PAA and H_2O_2, but a strong positive correlation between PAA and MHP, suggesting that the sinks of H_2O_2 were potentially different from those of MHP and PAA at Mazhuang site. Figure 9 depicts the hourly averaged concentrations of PAA, H_2O_2 and MHP, together with simultaneously measured concentrations of SO_2 and RH on 6 July at Mazhuang. The most striking feature is that H_2O_2 diurnal cycle was out of phase with MHP and PAA. Its concentrations were under detection limit during 07:00–11:00 LT and 17:00–19:00 LT, when SO_2 concentration was prevailing high; however, its concentrations remained a high level during 03:00–06:00 LT and 21:00–23:00 LT, indicating that the ozonolysis of alkenes possibly contributes to the production of H_2O_2 at night (Becker et al., 1990; Gäb et al., 1995; Grossmann et al., 2003; Möller, 2009). Since all the three peroxides have a common photochemical precursor, HO_2, and thus have a similar formation mechanism during the daytime, the unexpected profile of H_2O_2 in Mazhuang can be attributed to some removal processes, which probably have little impact on MHP and PAA. Considering a high level of SO_2, ~20 ppbv there, it is possible that a large portion of H_2O_2 was consumed by some reaction pathways, in which SO_2 was involved, although H_2O_2 was formed in a considerable amount. It is well known that the wet precipitation of peroxides, and their subsequent reactions with S(IV) in the aqueous phase are important pathways to remove them in the atmosphere (Reactions R12–R14).

$$H_2O_2 + HSO_3^- \rightarrow HSO_4^- + H_2O \tag{R12}$$

$$CH_3OOH + HSO_3^- \rightarrow HSO_4^- + CH_3OH \tag{R13}$$

$$CH_3C(O)OOH + HSO_3^- \rightarrow HSO_4^- + CH_3COOH \tag{R14}$$

The loss rate of PAA in the aqueous phase can be expressed as:

$$-\frac{d[\mathrm{PAA}]}{d[t]} = k[\mathrm{H}^+] \times [\mathrm{PAA}]_{\mathrm{aq}} \times [\mathrm{S(IV)}]_{\mathrm{aq}} \times V,$$

where k=$3.5\times10^7\,\mathrm{L}^2\,\mathrm{mol}^{-2}\,\mathrm{s}^{-1}$ (Lind et al., 1987), $[\mathrm{H}^+]$ was chosen as 1.0×10^{-5} M based on the pH values detected from rain samples at Mazhuang, V is the volume of liquid water and here we estimated its value as 8.0×10^{-7}–8.0×10^{-5} L $\mathrm{H_2O/m^3}$ air according to the local RH, $[\mathrm{PAA}]_{\mathrm{aq}}$ and $[\mathrm{S(IV)}]_{\mathrm{aq}}$ are aqueous-phase concentrations of PAA and S(IV), respectively, as calculated using the Henry's Law:

$$[\mathrm{PAA}]_{\mathrm{aq}}=\mathrm{H}_{\mathrm{PAA}}\times\mathrm{P}_{\mathrm{PAA}};\,[\mathrm{S(IV)}]_{\mathrm{aq}}=\eta\times\mathrm{H}_{\mathrm{SO_2}}\times\mathrm{P}_{\mathrm{SO_2}},$$

where $\mathrm{H}_{\mathrm{PAA}}$=$8.4\times10^2\,\mathrm{M\,atm}^{-1}$ (O'Sullivan et al., 1996), $\mathrm{H}_{\mathrm{SO_2}}$=$1.2\,\mathrm{M\,atm}^{-1}$ (Shorter et al., 1995), η is the ratio of the total dissolved S(IV) to the total dissolved $\mathrm{SO_2}$, and its value was calculated as 1330 at pH=5.

Accordingly, the loss rate of PAA due to its aqueous-phase oxidation of S(IV) can be calculated, as the function of relative humidity, gas-phase concentrations of $\mathrm{SO_2}$ and PAA. The total moles of PAA per cubic meter air, including both gas and aqueous phase, can be given by (Finlayson-Pitts and Pitts, 2000):

$$\text{Total PAA}=\frac{1000\times\mathrm{P}_{\mathrm{PAA}}}{\mathrm{RT}}+\mathrm{H}_{\mathrm{PAA}}\times\mathrm{P}_{\mathrm{PAA}}\times V$$

Thus, the loss rate of PAA due to its solubility and its aqueous-phase reaction with $\mathrm{SO_2}$ in $\%\,\mathrm{h}^{-1}$ is:

$$\frac{-d[\mathrm{PAA}]}{d[t]}/\text{Total PAA}$$

Similarly, the loss rates of $\mathrm{H_2O_2}$ and MHP were also obtained. As shown in Fig. 10, the low concentrations of peroxides coinciding with the high $\mathrm{SO_2}$ concentration and RH during 07:00–08:00 LT cause the loss rates of ~$0.7\%\,\mathrm{h}^{-1}$ for $\mathrm{H_2O_2}$, ~$1\times10^{-5}\%\,\mathrm{h}^{-1}$ for

MHP, and ~$7\times10^{-4}\%\,h^{-1}$ for PAA. Although the loss rate of H_2O_2 due to oxidizing S(IV) in the aqueous phase was several orders of magnitude higher than those of MHP and PAA, its value calculated is minor, resulting in that the aqueous-phase reaction between H_2O_2 and S(IV) can not sustain an efficient removal of H_2O_2, especially during the period of 08:00–10:00 LT and 17:00–19:00 LT, when the concentrations of H_2O_2 were expected to be much higher than observed, see Fig. 9. Apparently, there should be another sink of H_2O_2 maintaining its low level in the daytime. We suggest that the investigation of the reaction of H_2O_2 and S(IV) on the surface of water droplets may provide evidence to explain this unknown sink.

3.4 Implication on free radical chemistry

PAA can be considered as the reservoir of radicals. If PAA undergoes photochemical reactions, the radicals will be released, but if PAA undergoes the dry/wet deposition, it will certainly become a sink of radicals. Here we present a preliminary evaluation with respect to the influence of PAA on the radical budget using a box model with CBM-IV mechanism. The following two versions are implemented: Version-1 (including PAA kinetics) and Version-2 (excluding PAA kinetics). The initial VOCs and NO_x concentrations input were representative of average concentrations in early morning in Beijing-2006. The simulation was carried out on a 24-h basis and we chose the period from 24 h to 48 h for analysis. The modeling results in terms of the OH, HO_2 and $CH_3C(O)OO$ concentrations are shown in Fig. 11. There are three scenarios constrained by NO_x emissions: Scenario 1 (base case simulation), Scenario 2 (simulation with 20% NO_x emission decreased), and Scenario 3 (simulation with 50% NO_x emission decreased). Apparently, when PAA kinetics was applied to the CBM-IV mechanism, both HO_2 and $CH_3C(O)OO$ concentrations simulated would decrease correspondingly, and the extent of these two radicals undergoing PAA formation pathway depends on the NO_x level. Take the Scenario 3 as an example, PAA accounted for up to ~10% and ~20% homogeneous loss of HO_2 and $CH_3C(O)OO$, respectively, indicating that PAA is an important sink of HO_2 and $CH_3C(O)OO$ under low NO_x condition. In particular, the impact of PAA on $CH_3C(O)OO$ is much more evident than HO_2.

It is well known that the oxidation of VOCs by OH initiates radical cycling via HO_x (=$OH+HO_2$) and NO_x (=$NO+NO_2$) chemistry in the troposphere (Emmerson et al., 2007; Lelieveld et al., 2008; Sheehy et al., 2008; Dusanter et al., 2009; Hofzumahaus et al., 2009). Particularly speaking, the photo-chemical oxidation of some VOCs containing acetyl group generates $CH_3C(O)OO$, which can either react with NO_2 to form PAN, or react with NO and NO_3 to form CH_3O radicals in the polluted atmosphere (Tyndall et al., 2001). The CH_3O radical reacts with oxygen to produce HO_2, which will readily react with NO to generate recycled OH. However, in regions where NO_x levels are low, the fraction of $CH_3C(O)OO$ undergoing the above pathway will decrease because there is no sufficient NO_x to sustain the HO_x–NO_x cycling. As such, a significant amount of $CH_3C(O)OO$ and HO_2 will be removed due to the formation of PAA, leading to the termination of these radicals. The comparison between Version 1 and Version 2 indicates that PAA is potentially an important sink of $CH_3C(O)OO$ under low NO_x condition. To calculate the fraction of $CH_3C(O)OO$ undergoing PAA formation pathway in different regions, a more detailed mechanism constrained by the observed concentrations of various species is needed.

Very recently, the organic peroxy radicals and peroxides are found to be important intermediate species for explaining the OH radical missing source (Lelieveld et al., 2008) and the observed formation of organic aerosols (Paulot et al., 2009). Therefore, we think that the knowledge on PAA and other organic peroxides, in regard to their concentration, formation mechanism and role in the cycle of free radicals and the formation of secondary aerosols in the atmosphere is urgently needed.

4 Conclusions

Atmospheric PAA at both urban and rural sites of China were measured during the following five campaigns, namely, Beijing-2006, Beijing-2007, Beijing-2008, Backgarden-

2006, and Mazhuang-2007. PAA was often present at several-decade pptv level, with a maximum value of ~1 ppbv. Meteorological and chemical parameters in related to PAA are analyzed using the Principal Factor Analysis (PFA) method, indicating that its concentration will increase with enhancing temperature and total radiation, but decrease with enhancing SO_2, NO, NO_2, and relative humidity. The importance of various VOCs in terms of PAA formation potential is ranked using the maximum incremental reactivity (MIR) method, and the result shows that the acetyl-containing compounds, including dialkylbenzene, trialkylbenzene, isoprene, alkenes, and acetaldehyde, are important precursors of PAA. The contribution of PAN to the PAA formation is estimated on the basis of chemical kinetics. We find that when the NO/NO_2 concentration ratio is <0.2, PAN is an important contributor to PAA and the formation of PAA will have feedback on the existed $PAN-NO_x$ cycle by consuming acetyl peroxy radicals. The correlation between PAA and the other two peroxides (H_2O_2 and MHP) is analyzed. Evidence with regard to a potential sink of H_2O_2, which can not be effectively applied to MHP and PAA, under high SO_2 and relative humidity level conditions is provided. Finally, the influence of PAA on the radials budget is preliminarily accessed using a box model on the basis of CBM-IV mechanism. The simulation results suggest that under low NO_x level conditions, PAA can be regarded to an important sink of acetyl peroxy radicals. We suggest that the PAA scheme should be considered in the current chemical mechanism due to its impact on the HO_x and RO_x budget and the study for PAA kinetics constitutes important tasks in gaining insight into the free radical chemistry and the formation of secondary aerosols.

Acknowledgement. The authors gratefully thank the National Natural Science Foundation of China (grants 40875072 and 20677002), and the Project of Development Plan of the State Key Fundamental Research of MOST of China (grant 2005CB422203), for their financial support. The authors would like to thank L. M. Zeng group and M. Hu group (Peking University) for their O_3, SO_2, NO_x, and CO data and meteorological data; J. B. Zhang group (Peking University) for PAN data; S. J. Fan group (Sun Yet-sen University) for meteorological data; C. C. Chang group (Research Center of Environment Changes, Academia Sinica, Taiwan) for VOCs data; Y. Kondo group (Research Center for Advanced Science and Technology, the University of Tokyo) for

NO_x data; and A. Hofzumahaus group (Institute für Chemie and Dynamic der Geosphäre II: Troposphäre, Forschungszentrum Jülich) for HO_2 data.

References

Acker, K., Kezele, N., Klasinc, L., Möller, D., Pehnec, G., Šorgo, G., Wieprecht, W., and Žužul, S.: Atmospheric H_2O_2 measurement and modeling campaign during summer 2004 in Zagreb, Croatia, Atmos. Environ., 42, 2530–2542, 2008.

Atkinson, R., Baulch, D. L., Cox, R. A., Hampson Jr., R. F., Kerr, J. A., Rossl, M. J., and Troe, J.: Evaluated kinetic and photochemical data for atmospheric chemistry, organic species: supplement VII, J. Phys. Chem. Ref. Data, 28, 191–393, 1999.

Awad, M. I., Oritani, T., and Ohsaka, T.: Simultaneous potentiometric determination of peracetic acid and hydrogen peroxide, Anal. Chem., 75, 2688–2693, 2003.

Barth, M., Kim, S.-W., Skamarock, W., Stuart, W., Pickering, K. E., and Ott, L.: Simulations of the redistribution of formaldehyde, formic acid, and peroxides in the 10 July 1996 Stratospheric-tropospheric experiment: radiation, aerosols, and ozone deep convection storm, J. Geophys. Res., 112, D13310, doi:10.1029/2006JD008046, 2007.

Becker, K.-H., Brockmann, K. J., and Bechara, J.: Production of hydrogen peroxide in forest air by reaction of ozone with terpenes, Nature, 346, 256–258, 1990.

Carter, W. P. L. and Atkinson, R.: Computer modeling studies of incremental hydrocarbon reactivity, Environ. Sci. Technol., 23, 864–890, 1990.

Davies, D. M. and Deary, M. E.: Determination of peracids in the presence of a large excess of hydrogen peroxide using a rapid and convenient spectrophotometric method, Analyst, 113, 1477–1479, 1988.

Dodge, M. C.: Chemical oxidant mechanisms for air quality modeling: critical review, Atmos. Environ., 34, 2103–2130, 2000.

Dusanter, S., Vimal, D., Stevens, P. S., Volkamer, R., Molina, L. T., Baker, A., Meinardi, S., Blake, D., Sheehy, P., Merten, A., Zhang, R., Zheng, J., Fortner, E. C., Junkermann, W., Dubey, M., Rahn, T., Eichinger, B., Lewandowski, P., Prueger, J., and Holder, H.: Measurements of OH and HO_2 concentrations during the MCMA-2006 field campaign – Part 2: Model comparison and radical budget, Atmos. Chem. Phys., 9, 6655–6675, 2009, http://www.atmos-chem-phys.net/9/6655/2009/.

Effkemann, S., Brodsgaard, S., Mortensen, P., Linde, S.-A., and Karst, U.: Determination of gas phase peroxyacetic acid using pre-column derivatization with organic sulfide reagents and liquid chromatography, J. Chromatogr. A, 855, 551–561, 1999.

Emmerson, K. M., Carslaw, N., Carslaw, D. C., Lee, J. D., McFiggans, G., Bloss, W. J., Gravestock, T., Heard, D. E., Hopkins, J., Ingham, T., Pilling, M. J., Smith, S. C., Jacob, M., and Monks, P. S.: Free radical modelling studies during the UK TORCH Campaign in Summer 2003, Atmos. Chem. Phys., 7, 167–181, 2007, http://www.atmos-chem-phys.net/7/167/2007/.

Faust, B. C., Powell, K., Rao, C. J., and Anastasio, C.: Aqueous-phase photolysis of biacetyl, and a source of acetic acid, peroxyacetic acid, hydrogen peroxide, and the highly oxidizing peroxyacetyl radical in aqueous aerosols, fogs, and clouds, Atmos. Environ., 31, 497–510, 1997.

Fels, M. and Junkermann, W.: Occurrence of organic peroxides in air at a mountain site, Geophys. Res. Lett., 21, 793–796, 1993.

Finlayson-Pitts, B. J. and Pitts, J. N.: Chemistry of the Upper and Lower Atmosphere, Academic Press, New York, 2000.

Frey, M. M., Stewart, R. W., McConnell, J. R., and Bales, R. C.: Atmospheric hydroperoxides in West Antarctica: Links to stratospheric ozone and atmospheric oxidation capacity, J. Geophys. Res., 110, D23301, doi:10.1029/2005JD006110, 2005.

Gäb, S., Turner, W. V., Wolff, S., Becker, K. H., Ruppert, L., and Brockmann, K. J.: Formation of alkyl and hydroxyalkyl hydroperoxides on ozonolysis in water and in air, Atmos. Environ. 29, 2401–2407, 1995.

Gnauk, T., Rolle, W., and Spindler, G.: Diurnal variations of atmospheric hydrogen peroxide concentrations in Saxony (Germany), J. Atmos. Chem., 27, 79–103, 1997.

Grosjean, E., Grosjean, D., Woodhouse, L. F., and Yang, Y. J.: Peroxyacetyl nitrate and peroxypropionyl nitrate in Porto Alegre, Brazil, Atmos. Environ., 36, 2405–2419, 2002.

Grosjean, D.: Ambient PAN and PPN in southern California from 1960 to the SCOS97-NARSTO, Atmos. Environ., 37, S221–S238, 2003.

Grossmann, D., Moortgat, G. K., Kibler, M., Schlomski, S., Bachmann, K., Alicke, B., Geyer, A., Platt, U., Hammer, M. U., Vogel, B., Mihelcic, D., Hofzumahaus, A., Holland, F., and Volz-Thomas, A.: Hydrogen peroxide, organic peroxides, carbonyl compounds, and organic acids measured at Pabstthum during BERLIOZ, J. Geophys. Res., 108(D4), 8250, doi:10.1029/2001JD001096, 2003.

Hecht, G., Hery, M., Hubert, G., and Subra, I.: Simultaneous sampling of peroxyacetic acid and hydrogen peroxide in workplace atmospheres, Ann. Occup. Hyg., 48, 715–721, 2004.

Heikes, B. G., Lee, M., Bradshaw, J., and Sandholm, S.: Hydrogen peroxide and methylhydroperoxide distributions related to ozone and odd hydrogen over the North Pacific in the fall of 1991, J. Geophys. Res., 101, 1891–1905, 1996.

Hua, W., Chen, Z. M., Jie, C. Y., Kondo, Y., Hofzumahaus, A., Takegawa, N., Chang, C. C., Lu, K. D., Miyazaki, Y., Kita, K., Wang, H. L., Zhang, Y. H., and Hu, M.: Atmospheric hydrogen peroxide and organic hydroperoxides during PRIDE-PRD'06, China: their concentration, formation mechanism and contribution to secondary aerosols, Atmos. Chem. Phys., 8, 6755–6773, 2008, http://www.atmos-chem-phys.net/8/6755/2008/.

Hofzumahaus, A., Rohrer, F., Lu, K. D., Bohn, B., Brauers, T., Chang, C.-C., Fuchs, H., Holland, F., Kita, K., Kondo, Y., Li, X., Lou, S. R., Shao, M., Zeng, L. M., Wahner, A., and Zhang, Y. H.: Amplified trace gas removal in the troposphere, Science, 324, 1702–1704, 2009.

Jackson, A. V. and Hewitt, C. N.: Atmospheric hydrogen peroxide and organic hydroperoxides: a review, Environ. Sci. Technol., 28, 175–228, 1999.

Jenkin, M. E., Saunders, S. M., and Pilling M. J.: The tropospheric degradation of volatile organic compounds: a protocol for mechanism development, Atmos. Environ., 31, 81–104, 1997.

Johnson, R. M. and Siddiqi, I. W.: The Determination of Organic Peroxides, Pergamon, NewYork, 119 pp., 1970.

Jolliffe, I. T.: Principal Component Analysis. Springer, NewYork, 2002.

Keller, B. K., Wojcik, M. D., and Fletcher, T. R.: A directly-dissociative stepwise reaction mechanism for gas-phase peroxyacetic acid, J. Photoch. Photobio. A, 195, 10–22, 2008.

Lee, M., Heikes, B. G., and O'Sullivan, D. W.: Hydrogen peroxide and organic hydroperoxide in the troposphere: a review, Atmos. Environ., 34, 3475–3494, 1992.

Lelieveld, J., Butler, T. M., Crowley, J. N., Dillon, T. J., Fischer, H., Ganzeveld, L., Harder, H., Lawrence, M. G., Martinez, M., Taraborrelli, D., and Williams, J.: Atmospheric oxidation capacity sustained by a tropical forest, Nature, 452, 737–740, 2008.

Lind, J. A., Lazrus, A. L., and Kok, G. L.: Aqueous phase oxidation of sulfur by hydrogen peroxide and methyl hydroeroxide and peroxyacetic acid, J. Geophys. Res., 92, 4171–4177, 1987.

Lightfoot, P. D., Cox, R. A., Crowley, J. N., Destriau, M., Hayman, G. D., Jenkin, M. E., Moortgat, G. K., and Zabel, F.: Organic peroxyl radicals: kinetics, spectroscopy, and tropospheric chemistry, Atmos. Environ., 26A, 1805–1961, 1992.

McFadyen, G. G. and Cape, J. N.: Peroxyacetyl nitrate in eastern Scotland, Sci. Total Environ., 337, 213–222, 2005.

Mair, R. D. and Hall, R. T.: Determination of Organic Peroxides by Physical, Chemical, and Colorimetric Methods, Organic Peroxides Vol. 2, edited by: Swern, D., Wiley-Interscience, 535–635, 1970.

Möller, D.: Atmospheric hydrogen peroxide: evidence for aqueous-phase formation from an historic perspective and a one-year measurement campaign, Atmos. Environ., doi:10.1016/j.atmsenv.2009.08.013, in press, 2009.

Obermeyer, G., Aschmann, S. M., Atkinson, R., and Arey, J.: Carbonyl atmospheric reaction products of aromatic hydrocarbons in ambient air, Atmos. Environ., 43, 3736–3744, 2009.

Orlando, J. J., Tyndall, G. S., and Calvert, J. G.: Thermal-decomposition pathways for peroxylacetyl nitrate (PAN) – implications for atmospheric methyl nitrate levels, Atmos. Environ., 26, 3111–3118, 1992.

O'Sullivan, D. W., Lee, M., Noone, B. C., and Heikes, B. G.: Henry's law constant determinations for hydrogen peroxide, methyl hydroperoxide, hydroxymethyl hydroperoxide, ethyl hydroperoxide, and peroxyacetic acid, J. Phys. Chem., 100, 3241–3247, 1996.

Paulot, F., Crounse, J. D., Kjaergaard, H. G., Kürten, A., Clair, J. M. St., Seinfeld, J. H., and Wennberg, P. O.: Unexpected epoxide formation in the gas-phase photooxidation of isoprene, Science, 325, 730–733, 2009.

Pinkernell, U., Effkemann, S., Nitzsche, F., and Karst, U.: Rapid high-performance liquid chromatographic method for the determination of peroxyacetic acid, J. Chromatogr. A, 730, 203–208, 1996.

Reeves C. E. and Penkett, S. A.: Measurements of peroxides and what they tell us, Chem. Rev., 103, 5199–5218, 2003.

Ren, Y., Ding, A. J., Wang, T., Shen, X. H., Guo, J., Zhang, J. M., Wang, Y., Xu, P. J., Wang, X. F., Gao, J., and Collett, J. L. Jr.: Measurement of gas-phase total peroxides at the summit of Mount Tai in China, Atmos. Environ., 43, 1702–1711, 2009.

Ruttinger, H.-H. and Radschuweit, A.: Determination of peroxides by capillary zone electrophoresis with amperometric detection, J. Chromatogr. A, 868, 127–134, 2000.

Staffelbach, T. A., Orlando, J. J., Tyndall, G. S., and Calvert, J. G.: The UV-visible absorption spectrum and photolysis quantum yields of methylglyoxal, J. Geophys. Res., 100, 14189–

14198, 1995.

Sheehy, P. M., Volkamer, R., Molina, L. T., and Molina, M. J.: Oxidative capacity of the Mexico City atmosphere – Part 2: A ROx radical cycling perspective, Atmos. Chem. Phys. Discuss., 8, 5359–5412, 2008, http://www.atmos-chem-phys-discuss.net/8/5359/2008/.

Shorter, J. A., De Bruyn, W. J., Hu, J., Swartz, E., Davidovits, P., Worsnop, D. R., Zahniser, M. S., and Kolb, C. E.: Bubble column apparatus for gas-liquid heterogeneous chemistry studies, Environ. Sci. Technol., 29, 1171–1178, 1995.

Stockwell, W. R.: The effect of gas-phase chemistry on aqueous-phase sulphur dioxide oxidation rate, J. Atmos. Chem., 19, 317–329, 1994.

Tyndall, G. S., Cox, R. A., Granier, C., Lesclaus, R., Moortgat, G. K., Pilling, M. J., Ravishankara, A. R., and Wallington, T. J.: Atmospheric chemistry of small organic peroxy radicals, J. Geophys. Res., 106(D11), 12157–12182, 2001.

Volkamer, R., Sheehy, P. M., Molina, L. T., and Molina, M. J.: Oxidative capacity of the Mexico City atmosphere – Part 1: A radical source perspective, Atmos. Chem. Phys. Discuss., 7, 5365–5412, 2007, http://www.atmos-chem-phys-discuss.net/7/5365/2007/.

Walcek, C. J.: A theoretical estimated of O_3 and H_2O_2 dry deposition over Northeastern United States, Atmos. Environ., 21, 2649–2659, 1987.

Walker, S. J., Evans, M. J., Jackson, A. V., Steinbacher, M., Zellweger, C., and McQuaid, J. B.: Processes controlling the concentration of hydroperoxides at Jungfraujoch Observatory, Switzerland, Atmos. Chem. Phys., 6, 5525–5536, 2006, http://www.atmos-chem-phys.net/6/5525/2006/.

Wesley, M. L.: Parameterization of surface resistances to gaseous dry deposition in regional scale numerical models, Atmos. Environ., 23, 1293–1304, 1989.

Xie, X., Shao, M., Liu, Y., Lu, S. H., Chang, C. C., and Chen, Z. M.: Estimate of initial isoprene contribution to ozone formation potential in Beijing, China, Atmos. Environ., 42, 6000–6010, 2008.

Xu, J. R. and Chen, Z. M.: Determination of peroxides in environmental samples by high performance liquid chromatography with fluorescence detection, Chinese J. Chromatogr., 23, 366–369, 2005.

Yang, Y. J., Stockwell, W. R., and Milford, J. B.: Uncertainties in incremental reactivities of volatile organic compounds, Environ. Sci. Technol., 29, 1336–1345, 1995.

Table 1. The rotated factor matrix from principal factor analysis of data at Backgarden 2006 (*n*=317; accumulative variance 71.8%).

Factor	1	2	3	4
PAA	**0.53**	−0.12	**−0.49**	0.10
SO_2	−0.33	**0.80**	0.14	0.31
NO	−0.19	0.14	0.02	**0.73**
NO_2	**−0.50**	**0.58**	−0.25	0.05
CO	**−0.57**	0.39	−0.14	−0.23
O_3	**0.71**	0.42	0.21	−0.04
WD	**0.62**	0.18	−0.39	−0.05
WS	−0.14	−0.49	**0.51**	0.45
T	**0.86**	0.41	0.08	−0.05
RH	**−0.88**	−0.27	−0.22	0.01
TI	**0.64**	0.09	**0.58**	0.09
P	−0.35	0.01	**0.61**	−0.49
Variance explained	34.7%	15.5%	12.7%	8.9%

Fig. 1. Map showing the location of observation sites, Beijing, Mazhuang and Backgarden.

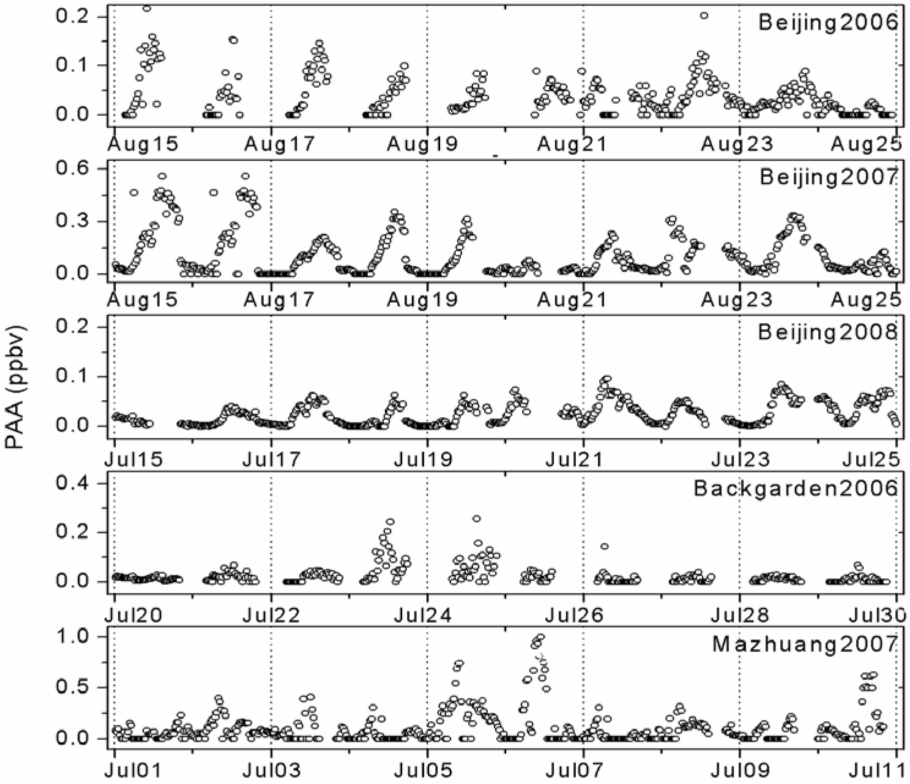

Fig. 2. Temporal profiles of atmospheric PAA concentrations during periods of five campaigns.

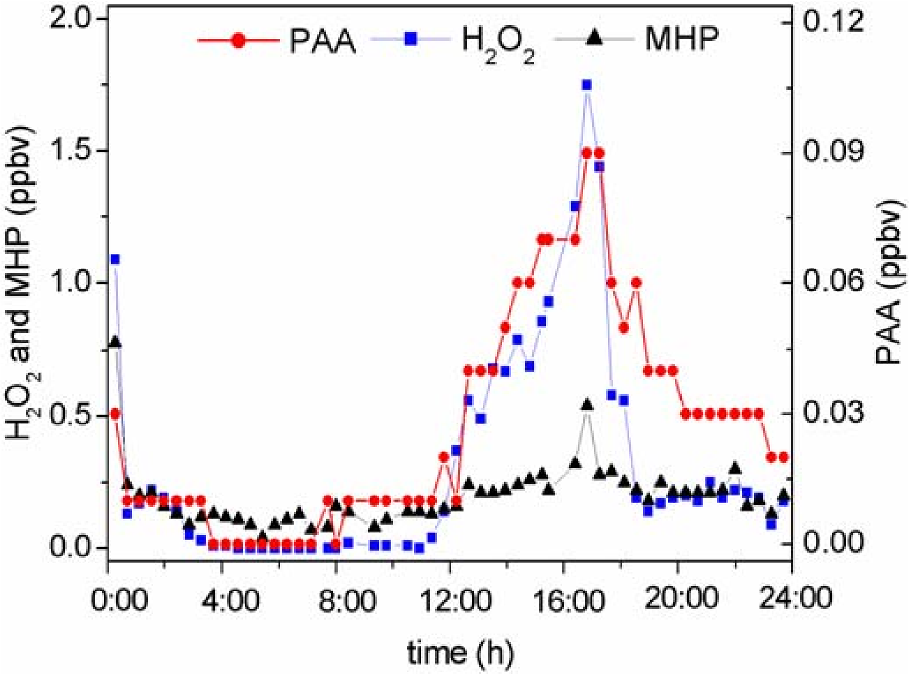

Fig. 3. Diurnal cycle for PAA, H_2O_2, and MHP in Beijing on 2 August 2008.

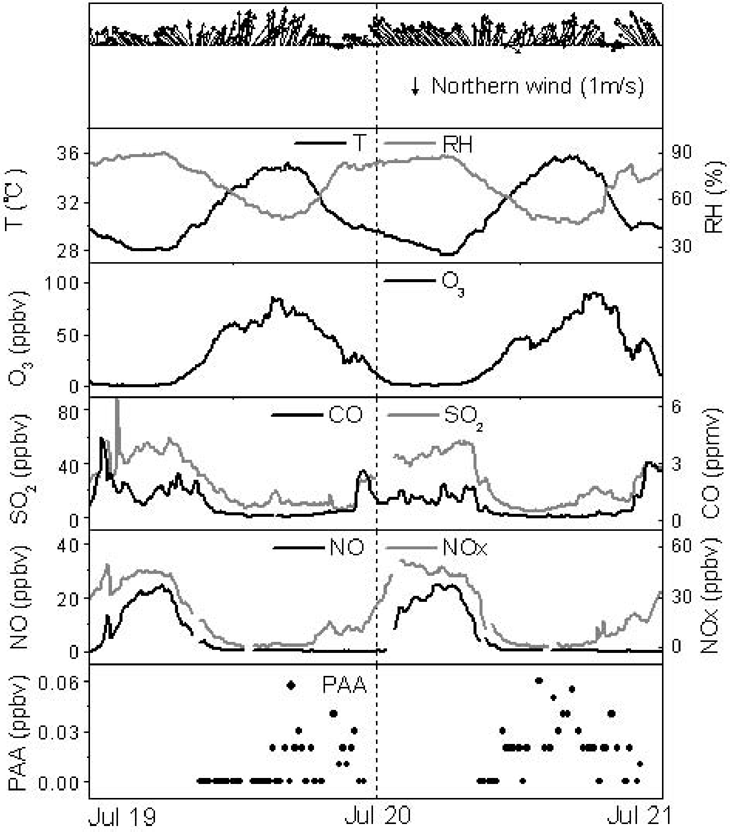

Fig. 4. Diurnal profiles of wind speed, wind direction, temperature, relative humidity, CO, SO_2, NO, O_3, and PAA at Backgarden from 19 to 20 July 2006.

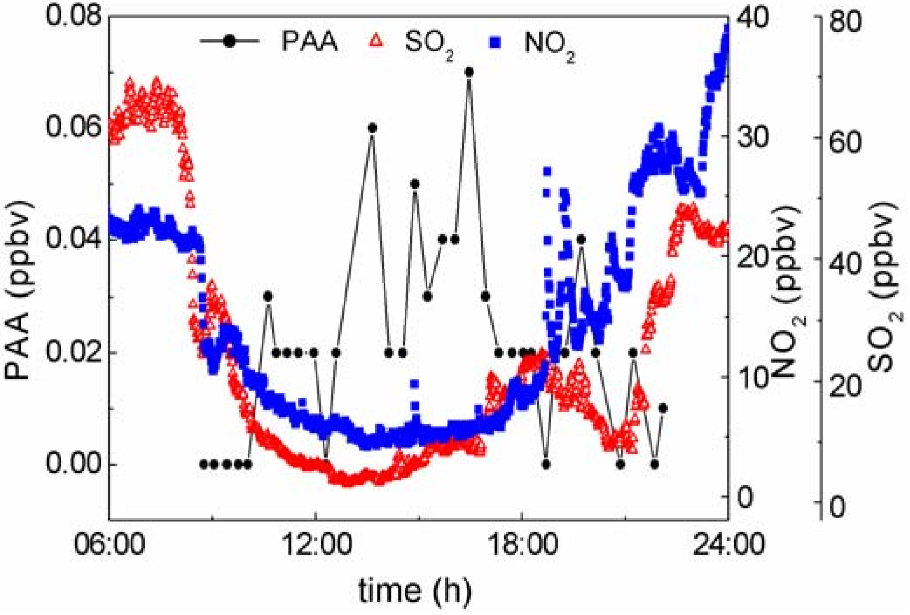

Fig. 5. Diurnal profiles of PAA, SO_2, and NO_2 at Backgarden on 21 July 2006.

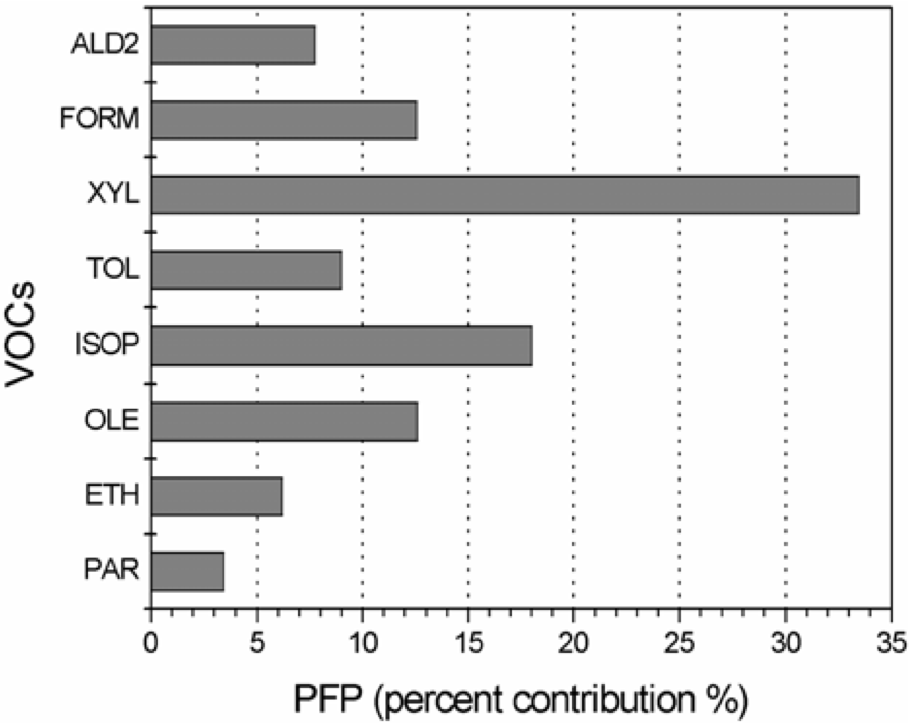

Fig. 6. Percent contribution (%) of VOCs to the PAA formation potential.

Title Page
Abstract
Introduction
Conclusions
References
Tables
Figures
◀▮
▶▮
◀
▶
Back
Close
Full Screen / Esc
Printer-friendly Version
Interactive Discussion

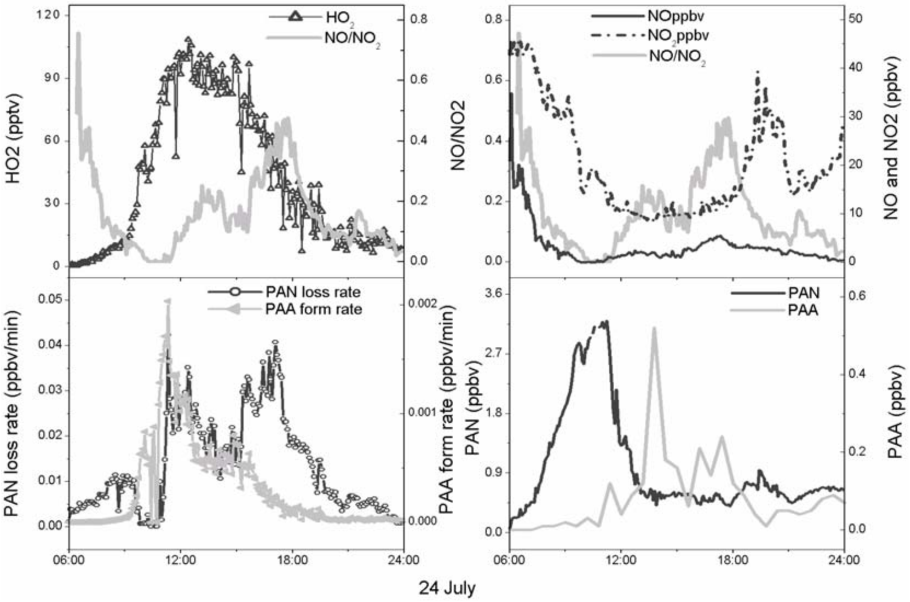

Fig. 7. Diurnal variations of PAN loss rate, PAA formation rate, together with concentrations of PAA, PAN, NO, NO_2 and HO_2 at Backgarden on 24 July 2006.

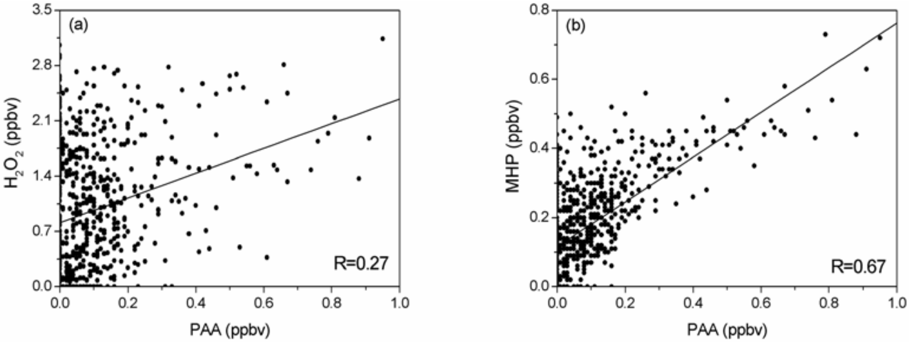

Fig. 8. Hourly averaged scatter plots of PAA vs. H_2O_2 and PAA vs. MHP at Mazhuang in July 2007.

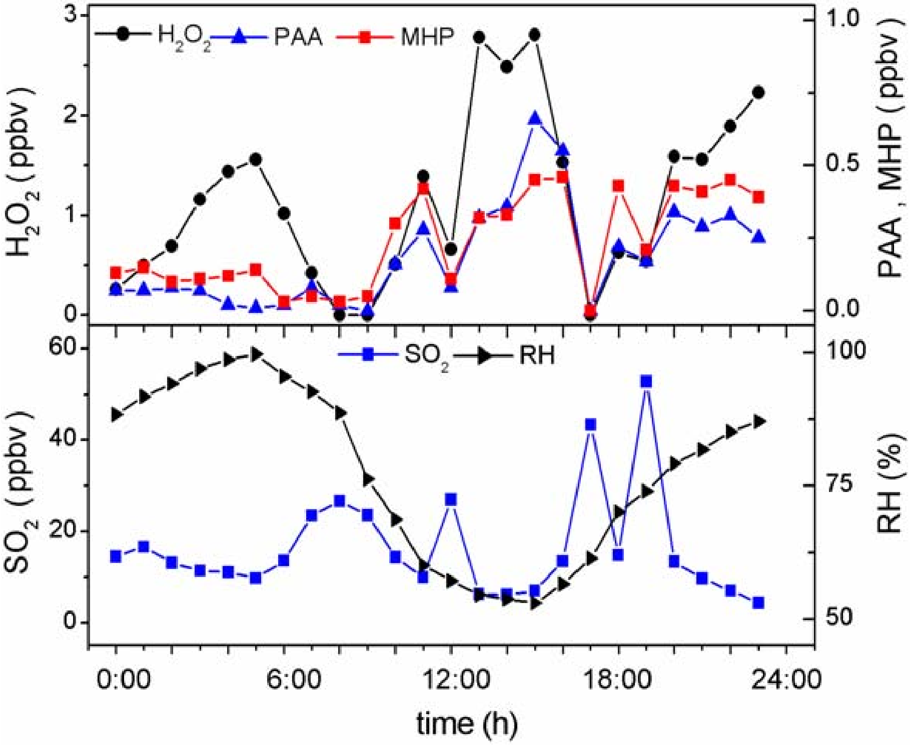

Fig. 9. Hourly averaged diurnal cycle for PAA, H_2O_2, MHP, SO_2 and RH at Mazhuang on 6 July 2007.

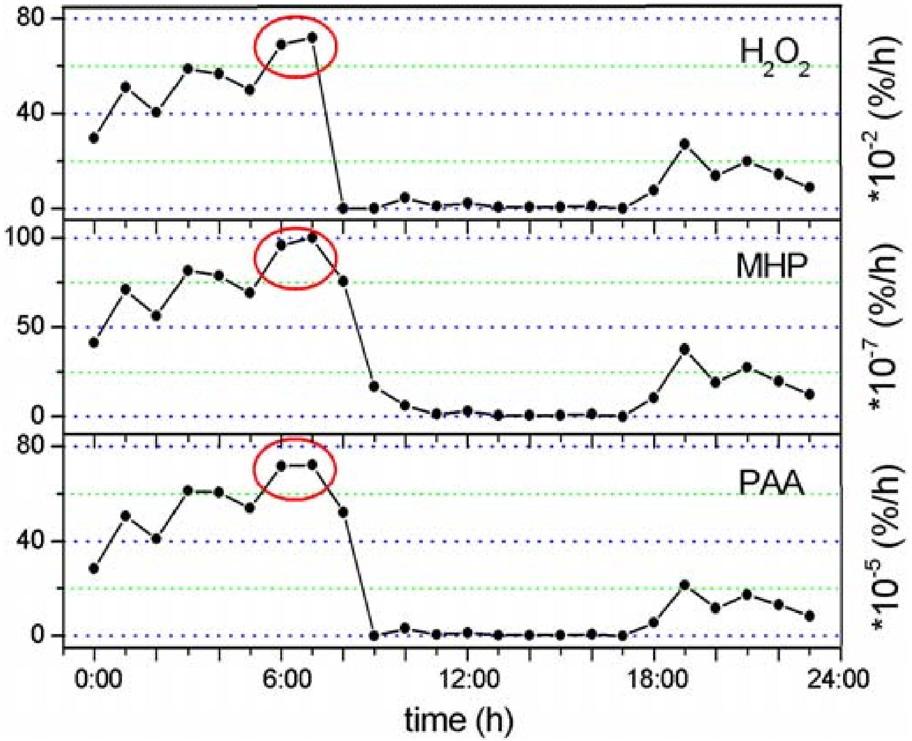

Fig. 10. Aqueous-phase loss rates of H_2O_2, MHP, and PAA in percent per hour derived from data at Mazhuang on 6 July 2007.

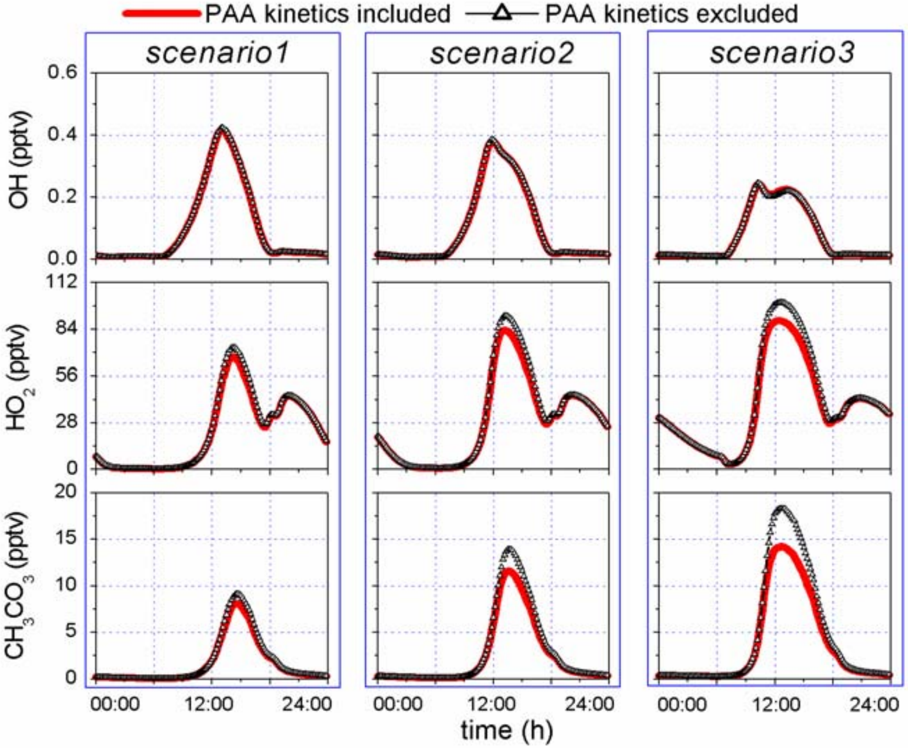

Fig. 11. The box model simulation of concentrations of free radicals before and after the PAA kinetics added to the CBM-IV mechanism (scenario 1 represents the base case simulation; scenario 2 represents the simulation with 20% NO_x emission decreased; scenario 3 represents the simulation with 50% NO_x emission decreased).